Fluorescent Microtubules Break Up under Illumination

G. P. A. Vigers, M. Coue, and J. R. McIntosh

Department of Molecular, Cellular, and Developmental Biology, University of Colorado at Boulder, Boulder, Colorado 80309

Abstract. We have synthesized three new fluorescent analogues of tubulin, using fluorescein or rhodamine groups attached to *N*-hydroxy-succinimidyl esters, and have partially characterized the properties of these analogues. We have also further characterized the tubulin derivatized with dichlorotriazinyl-aminofluorescein that has previously been used in this and other laboratories. Our results show that all four analogues assemble into microtubules which break up when exposed to light of the wavelengths that excite fluorescence. This sensitivity places severe constraints on the use of these analogues in studies of microtubule dynamics.

MUCH information has been gained about the dynamic distribution of tubulin in living cells through the use of tubulin tagged with a fluorescent molecule and injected into cultured cells (Keith et al., 1981; Wadsworth and Sloboda, 1983; Salmon et al., 1984*a*; Saxton et al., 1984; Soltys and Borisy, 1985; Gorbsky et al., 1987; Saxton and McIntosh, 1987). The dynamics of the tubulin can then be followed either by watching the incorporation of the fluorescent analogue immediately after injection, or by monitoring its fluorescence redistribution after photobleaching (FRAP).[1] It has been hoped that this latter method will give a more faithful report on the steady-state behavior of the cell, since the cell can be allowed to recover from any injection trauma and from the change in cellular tubulin levels caused by injection (Saxton et al., 1984). However, both methods clearly rely on the assumption that the fluorescently labeled tubulin reports faithfully the behavior of the cell's unlabeled tubulin, at least to the accuracy of the methods used to track the fluorescence and at the concentrations of labeled tubulin injected.

For this reason, considerable effort has been expended to find good fluorescent tubulin analogues and to characterize their properties. Until recently, the best analogue available appeared to be dichlorotriazinyl-aminofluorescein tubulin (DTAF-tubulin) (Keith et al., 1981; Wadsworth and Sloboda, 1983; Leslie et al., 1984). However, new fluorescent reagents have recently become available, including an amine-selective succinimidyl linkage, which allow one to prepare new fluorescent derivatives of tubulin. With these we have made fluorescein, rhodamine, and X-rhodamine derivatives of tubulin, all of which contain a succinimidyl linkage group. This group is presumably attached to one of the accessible amines of the protein. These analogues all have a higher fluorescence-to-protein (f-to-p) ratio and better in vitro assembly characteristics than the DTAF-tubulin previously used. They also generally have less noncovalently bound dye. These fluorescent analogues have been injected into cultured PtK1 cells, where they all incorporate into the microtubule (MT) cytoskeleton of the cells. However, our results suggest that both these analogues and the DTAF-tubulin previously used suffer from a major problem: microtubules formed from them, either in vitro or in vivo, are destroyed as the bound fluorophore becomes photobleached. In this paper, we characterize the photolability of the fluorescent microtubules and provide information on the factors that modulate it. We also discuss the limitations that this phenomenon poses on conclusions that may be drawn from studies that use fluorescent tubulins.

Materials and Methods

Preparation of Fluorescent Tubulins

Tubulin was labeled with DTAF, 5(6) carboxy fluorescein succinimidyl ester (NHS-Fl), 5(6) carboxyrhodamine B succinimidyl ester (NHS-Rh), or 5(6) carboxy-X-rhodamine succinimidyl ester (NHS-XRh). The same labeling procedure was used in all cases: phosphocellulose-purified tubulin (PC tubulin; Williams and Lee, 1982) was polymerized at a concentration of 4 mg/ml for 30 min at 37°C in a buffer containing 3.7 M glycerol, 50 mM Pipes, 50 mM Hepes at pH 7.3, 1 mM EGTA, 10 mM $MgSO_4$ and 1 mM GTP. The fluorescent dye was dissolved in DMSO and mixed rapidly with the protein at a final dye-to-tubulin ratio of 40:1 (final DMSO concentration <5%). After an incubation of 30 min at 37°C with occasional gentle mixing, the microtubule solution was desalted on a Sephadex G-25 column to remove most of the unbound dye, using a column buffer containing 1 M Na-glutamate at pH 7.0, 1 mM EGTA, 0.1 mM GTP. The fluorescent proteins were depolymerized on ice for 20 min and the cold stable aggregates removed by centrifugation at 125,000 *g* at 4°C for 30 min. The supernatant was brought to 1 mM GTP and polymerized at 37°C for 30 min. Microtubules were pelleted at 125,000 *g* at 37°C for 40 min and resuspended in the glutamate buffer. The cycle of depolymerization and repolymerization was

1. *Abbreviations used in this paper*: DIC microscopy, differential interference contrast microscopy; DTAF, 5-(4,6 dichlorotriazinyl) aminofluorescein; FRAP, fluorescence redistribution after photobleaching; f-to-p ratio, fluorescence-to-protein ratio; MAP, microtubule-associated protein; MJ, megajoule; MT, microtubule; MW, megawatt; NHS-Fl, 5(6) carboxyfluorescein succinimidyl ester; NHS-FTb, 5(6) carboxyfluorescein succinimidyl tubulin; NHS-Rh, 5(6) carboxyrhodamine B succinimidyl ester; NHS-RTb, 5(6) carboxyrhodamine succinimidyl tubulin; NHS-XRh, 5(6) carboxy-X-rhodamine succinimidyl ester; NHS-XRTb, 5(6) carboxy-X-rhodamine succinimidyl tubulin; PC tubulin, phosphocellulose-purified tubulin; T_c, time to dissolution; T_i, time of illumination.

repeated once and the final microtubule pellet was resuspended in an injection buffer consisting of 10 mM glutamic acid, 140 mM KOH, 20 mM citric acid, 1 mM $MgSO_4$, 1 mM EGTA, and 0.1 mM GTP at pH 7.0. After a final cold spin for clarification, the protein concentration of the supernatant was ~4 mg/ml and the final yield of fluorescent tubulin was 15–20%. The purity of the fluorescent tubulin and the amount of free or noncovalently bound dye was analyzed by SDS-PAGE according to Laemmli (Laemmli, 1971).

The molar f-to-p ratio of the final product was estimated by measuring protein concentration with the method of Bradford (1976) and dye concentration with a spectrophotometer, using extinction coefficients of 57,000 at 495 nm for DTAF, 48,000 at 495 nm for NHS-Fl, 66,000 at 560 nm for NHS-Rh, and 70,000 at 587 nm for NHS-XRh. These extinction coefficients were measured from solutions of the unbound dyes in a buffer containing 50 mM Pipes at pH 6.9, 1 mM EGTA, 1 mM $MgSO_4$, 1 mM GTP (PME buffer).

Polymerization Measurements

Tubulin assembly kinetics were followed by turbidometry at 350 nm in a spectrophotometer (model Lambda 4B; Perkin-Elmer Corp., Pomona, CA) with a thermostated sample chamber. The self-assembly kinetics of labeled or unlabeled tubulin at 1–2 mg/ml were measured in the presence of heat-stable microtubule-associated proteins (MAPs), prepared from bovine brain as previously described (Leslie et al., 1984). MAPs were used at 0.2 mg/ml at 37°C in PME buffer. The steady-state critical concentrations of labeled and unlabeled tubulin were determined by diluting a stock solution of polymerized microtubules (1.4 mg/ml) in a buffer containing 50 mM Pipes, 10 mM $MgSO_4$, 1 mM EGTA, 1 mM GTP, 3.4 M glycerol, pH 6.9. The absorption at 350 nm of each sample was measured after 2–3 h incubation at 37°C.

Optics

Fluorescence imaging was performed on a Zeiss Universal Microscope equipped with a 200-W mercury arc lamp and epifluorescence optics. The image was recorded with a camera (series 66 ISIT; DAGE MTI, Inc., Wabash, MI), and successive video frames were averaged and stored on an IRIS computer equipped with image processing hardware assembled by Hannaway and Associates, Boulder, CO. We have found that the best objective lens available for this type of fluorescence imaging is the 100× 1.25 NA plan objective (Carl Zeiss, Inc., Thornwood, NY). This lens has a very symmetrical point spread function above and below focus, and thus gives a minimum contribution to the image from objects outside the plane of focus. The field of view of the objective lens is not flat, but only the central part of the field is imaged by the ISIT camera, so this limitation is unimportant. This lens also has a very high brightness factor, due to its high numerical aperture and small number of lens elements. It is therefore well suited to low light level imaging of dim objects. The epifluorescence illumination intensity was varied between 7 and 300 kW/m^2.

Differential interference contrast (DIC) microscopy was performed on the same Zeiss Universal microscope, with a Zeiss 100× plan objective, Zeiss-Nomarski optics, and a DAGE MTI 67 video camera. The epifluorescence filter pack was retained in the optical path, above the Nomarski analyzer, so that the beam from a 2-W argon-ion laser (Spectra-Physics Inc., Mountain View, CA) could be introduced into the light train of the microscope through the epifluorescence filter pack and used to irradiate the specimen during DIC observation. The intensity of laser irradiation was measured with a laser power meter (Epply Laboratory Inc., Newport, RI) and was varied between 1 and 280 megawatt $(MW)/m^2$, using neutral density filters. To observe the MTs without illuminating them with damaging light, the light from the arc lamp was passed through a heat filter and a narrow-band, pass, green (546-nm) interference filter, and the MTs were observed through a fluorescein epifluorescence filter pack whose transmission band matched that of the interference filter in the illumination pathway. This wavelength of illumination produced no measurable dissolution of the fluorescein-labeled MTs, but laser light of a chosen (damaging) wavelength could also be introduced through the epiillumination pathway to irradiate the MTs.

The time taken for the MTs to "disappear" was taken as the time when the fragments of the MTs visible by DIC optics ceased to be distinguishable from the background (see Fig. 3). In a series of trials, the times to dissolution were judged independently by two operators to within ~2%, which was considerably less than the variability caused by other factors in the experiment (see Results).

The pictures shown in Figs. 4 and 5 were obtained using a different Zeiss Universal microscope, equipped with slightly superior DIC optics, no intervening fluorescence filter pack, and a DAGE MTI 68 video camera. The MTs were illuminated with light from a 100-W mercury arc lamp and the images were recorded on a Super-VHS video tape recorder (Mitsubishi International Corp., New York, NY).

Since our laser would not emit at wavelengths >514.5 nm, we could not use it to excite rhodamine fluorescence efficiently. The bulk of the data reported here were therefore collected on MTs composed of succinimidyl fluorescein tubulin. Comparisons between fluorescein- and rhodamine-labeled MTs were made using illumination from the 100-W Hg arc lamp and the appropriate filters. All data were collected at 26°C on MTs stabilized with 10 μM taxol unless otherwise stated.

Results

Purification of Fluorescent Tubulin and Removal of Unbound Dye

In the process of preparing DTAF-tubulin by the method previously described (Leslie et al., 1984) we realized that our final product contained a considerable amount of unbound dye. This dye ran well in front of the bromophenol blue–dye front in our gels, and in the environment of the gel it was only weakly fluorescent when compared to dye bound to protein (cf. Fig. 3). It was therefore not visualized if the gels were run to completion. To improve the purity of the DTAF-tubulin we added a Sephadex G25 column purification to the labeling procedure, as described under Materials and Methods. The new procedure yielded a DTAF-tubulin with much less unbound dye, but the f-to-p ratio of the product was ~0.1. A systematic variation of labeling conditions failed to produce DTAF-tubulin with a higher f-to-p ratio, so we experimented with other fluorescent tags. Besides DTAF, we used NHS-Fl, NHS-Rh, and NHS-XRh. Fig. 1 shows the purity of the NHS-Fl tubulin we obtained. At the end of the purification there was no detectable free dye associated with the fluorescent tubulin and the f-to-p ratio was ~0.5. The two rhodamine dyes yielded a final tubulin product with about the same apparent f-to-p ratio, but the true f-to-p ratios of these preparations were difficult to estimate because they still contained some unbound dye after two cycles of polymerization and depolymerization. We believe this is related to the hydrophobic character of the rhodamine dyes.

The labeling of tubulin with NHS-Fl, NHS-Rh, or NHS-XRh under the conditions used did not seem to affect its assembly properties significantly. In the presence of heat-stable MAPs, labeled and unlabeled tubulin show similar rates of assembly (Fig. 2 *A* for succinimidyl fluorescein tubulin [NHS-FTb]; and data not shown for the rhodamine tubulins). The critical concentration for assembly, determined at steady state, was the same for NHS-Fl tubulin and for unmodified tubulin (Fig. 2 *B*). Finally, all three fluorescent analogues copolymerized with unlabeled tubulin (see below, Figs. 3 and 4).

Behavior of the Fluorescent Tubulins After Microinjection

The fluorescent tubulins were injected into cells, where they appeared to incorporate rapidly into MT networks, as visualized by direct fluorescence imaging (see Fig. 3). However, during continued observation of the injected cells the MT networks of the cells appeared to dissolve. Fig. 3, *A* and *B*, shows cells injected with succinimidyl-B-rhodamine tubulin (NHS-RTb) and illuminated with green (546-nm) light. The

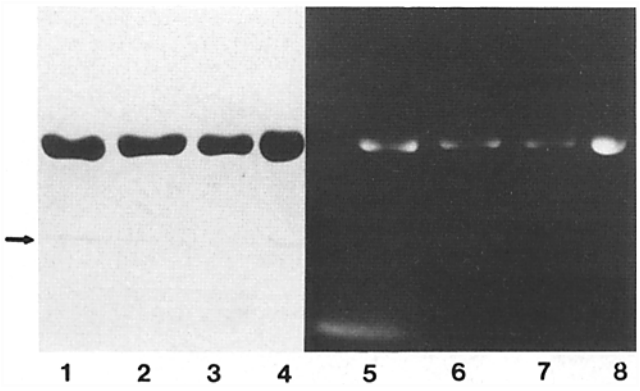

Figure 1. SDS-PAGE of the major steps in the preparation of NHS-Fl tubulin. Lanes *1–4*, Coomassie staining. Lanes *5–8*, fluorescent image of the gel. Lanes *1* and *5*, preparation after G25 desalting column. Note the fluorescence due to unbound dye running in front of the bromophenol blue–dye front (*arrow*). Apparent f-to-p ratio, 3.5. Lanes *2* and *6*, cold high-speed supernatant after centrifugation of the G25 fraction. Lanes *3* and *7*, cold high-speed supernatant after the first cycle of assembly and disassembly. Lanes *4* and *8*, final NHS-FTb corresponding to the cold supernatant after the second cycle of assembly and disassembly. No free dye is apparent in the final product. F-to-p ratio, 0.5.

MT networks within the cells appear to dissolve within 3 min under the conditions used, even though they have only been exposed to light for a total of ~6 s. Note that the MT network has disappeared before all of the fluorescence has been bleached. Fig. 3 *C* shows that the same effect is seen with NHS-FTb, but in this case the change in the network seems to be much reduced. Since fluorescein is more photolabile than rhodamine under our conditions (see below), and since the cell was irradiated while it was selected and brought into focus, the networks containing NHS-FTb are probably already dissolving by the time of the first picture in the series, thus reducing the magnitude of the subsequent change. The effect also appeared to vary somewhat between cells and between different areas of the same cell for reasons that were unclear. To investigate the problem further, and to determine more precisely what was happening to the MTs under different experimental conditions, we examined the behavior of the MTs in vitro using DIC microscopy.

Observations In Vitro by DIC Microscopy

Fluorescent MTs are Photolabile In Vitro, Regardless of the Fluorophore Used. Fluorescently labeled MTs were polymerized in PME buffer containing 10 μM taxol and viewed in the DIC microscope under continuous illumination with white light from a 100-W Hg arc lamp, as described in Materials and Methods. In all cases the MTs were initially well defined and indistinguishable from MTs assembled from unlabeled tubulin. During observation, however, the MTs appeared to break at random time intervals and at random positions along their lengths, getting shorter and shorter until they could no longer be seen in the DIC microscope. Control samples of MTs assembled from unlabeled PC tubulin in taxol did not show this effect at all. Fig. 4 *A* shows a sample of NHS-XRTb; the MTs fragment completely in ~250 s. Fig. 4 *B* shows similar behavior of NHS-RTb MTs, which break up in ~120 s under the same conditions. Fig. 4 *C* shows the same behavior for NHS-FTb MTs, which break up in ~40 s. By using interference filters in the illumination path, we were able to show that the NHS-FTb MTs are stable under green (546-nm) light for >600 s but disappear under blue (435-nm and longer) light in 40 s. Conversely, the NHS-RTb MTs are

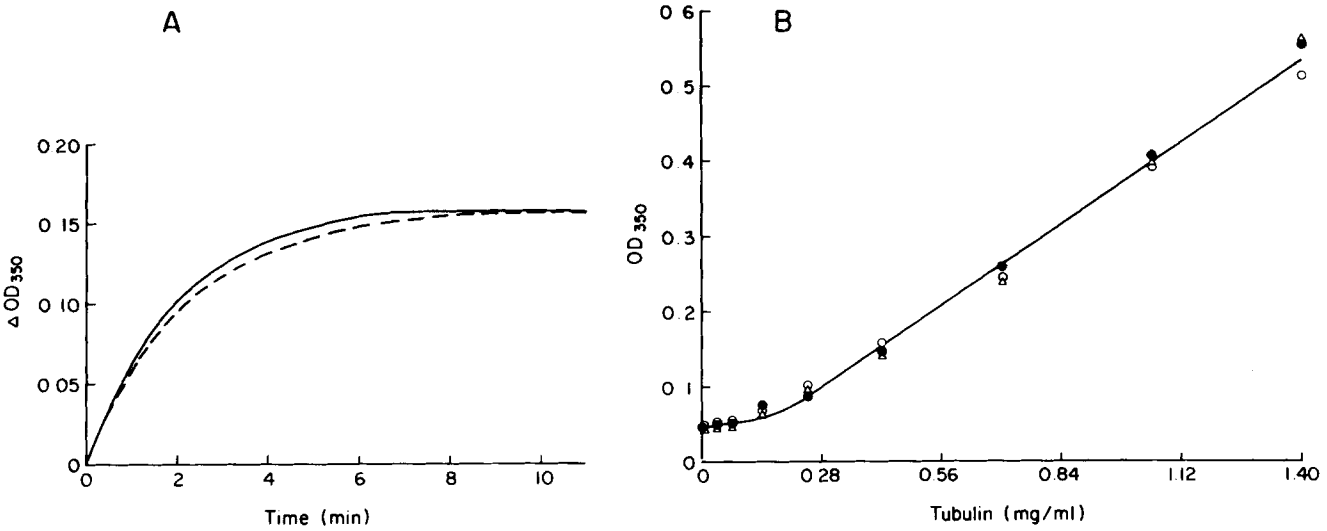

Figure 2. Polymerization properties of NHS-FTb. (*A*) Assembly kinetics of NHS-FTb (---) and unlabeled PC tubulin (——) at a concentration of 2 mg/ml in PME buffer and in the presence of 0.2 mg/ml heat-stable MAPs. The assembly was induced by a shift of temperature from 10 to 37°C and monitored by following the increase of turbidity at 350 nm. After steady state was achieved, the solution was incubated at 4°C to confirm that the increase in turbidity represented polymer formation and was fully reversible by cold treatment (data not shown). (*B*) Determination of the critical concentrations of the NHS-FTb and of unlabeled PC tubulin. Stock solutions at 1.4 mg/ml of unlabeled PC-tubulin (○) and NHS-FTb with an f-to-p ratio of 0.25 (●) or 0.5 (△) were polymerized at 37°C in PME buffer. The MT solutions were then diluted serially in the same buffer. The turbidity of each sample was measured after 2–3 h incubation at 37°C. The same critical concentration (~0.18 mg/ml) was obtained for unlabeled tubulin and the NHS-FTbs, irrespective of f-to-p ratio.

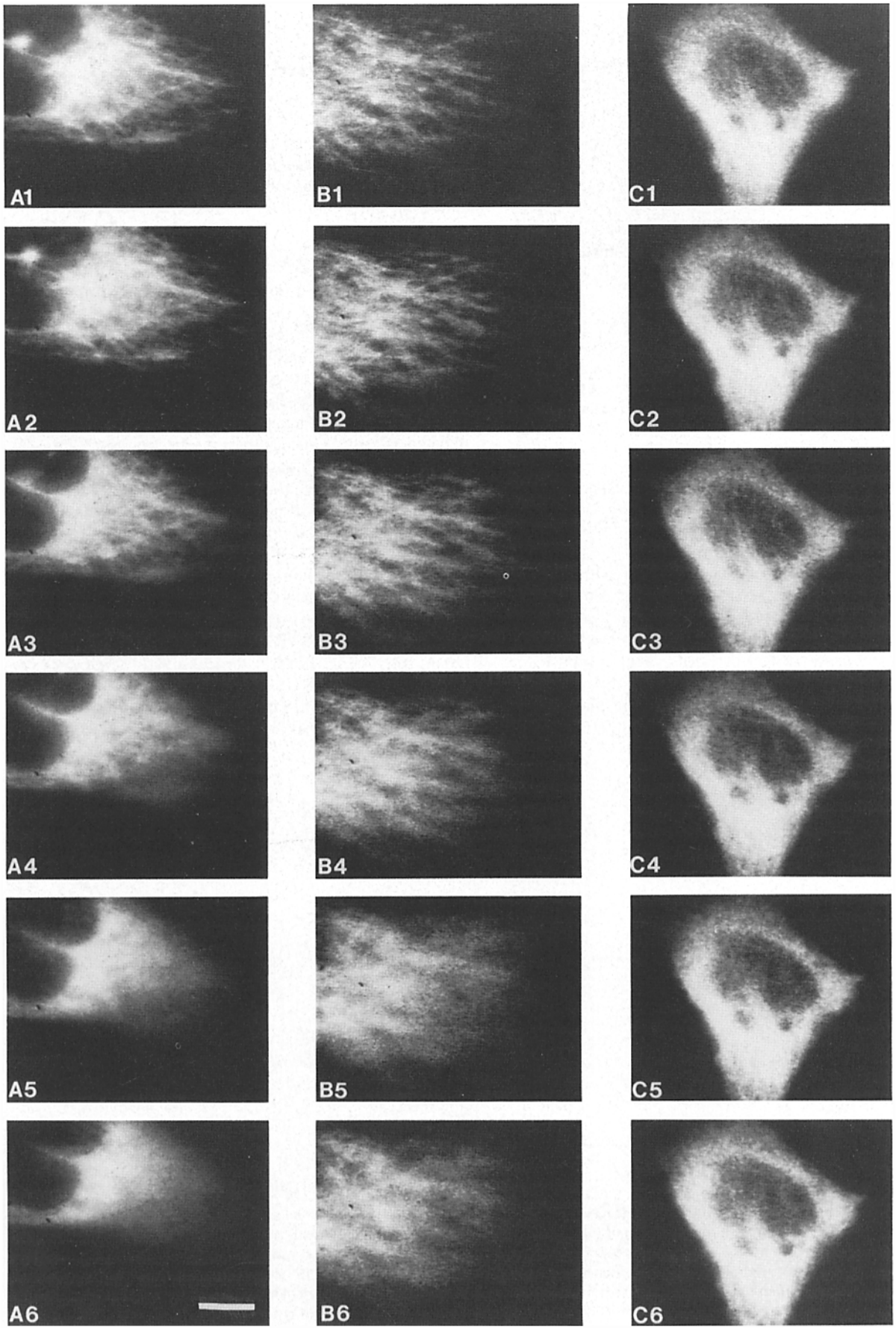
A1
B1
C1
A2
B2
C2
A3
B3
C3
A4
B4
C4
A5
B5
C5
A6
B6
C6

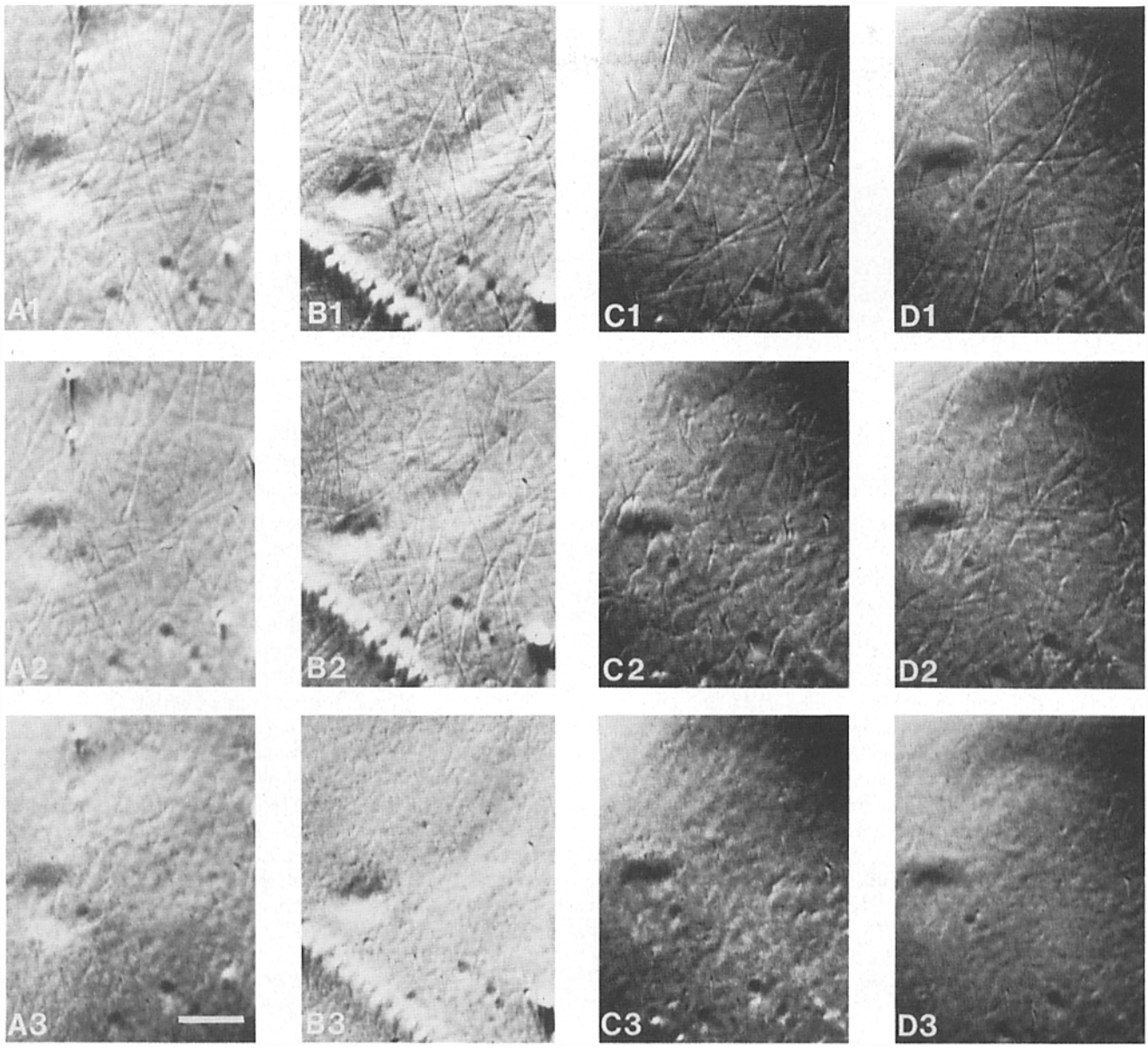

Figure 4. DIC images of microtubules in vitro. NHS-XRTb with an f-to-p ratio of ~0.5 (*A*), NHS-RTb with an f-to-p ratio of ~0.5 (*B*), and NHS-FTb with an f-to-p ratio of 0.5 (*C*) or 0.25 (*D*) were polymerized in the presence of 10 μM taxol at 2 mg/ml in PME buffer. The resulting MTs were observed on a DIC microscope under green (*A* and *B*) or blue (*C* and *D*) light at 26°C with continuous illumination from a 100-W Hg arc lamp (see Materials and Methods). Time between photographs, (*A*) 120 s, (*B*) 60 s, (*C*) 20 s, and (*D*) 60 s. Bar, 10 μm.

stable under blue light for >600 s, but dissolve under green light in 250 s. Thus the dissolution of fluorescent MTs only occurs at wavelengths which excite the fluorescent moiety on the tubulin used (see also below). The different times required for the MTs to break up in Fig. 4, *A–C*, probably reflect both the different susceptibilities of the fluorescent tubulins to dissolution, and the different light intensities delivered by the arc lamp at different wavelengths.

Photodestruction of MTs is Irreversible, but Not Contagious. The area of the glass denuded of MTs was examined

Figure 3. Injected cells. PtK1 cells were grown on glass coverslips and microinjected with succinimidyl rhodamine tubulin (*A* and *B*) or succinimidyl fluorescein tubulin (*C*). After incubation at 37°C in an incubator for >2 h, the coverslips were mounted on microscope slides and illuminated with green (*A* and *B*) or blue (*C*) light. Cells were selected, focused, and imaged in epifluoroescence under illumination from a 200-W mercury arc lamp. *A*, *1–6*, was exposed under maximum illumination from the green line of the arc lamp (~300 kW/m^2), while *B*, *1–6*, was exposed at minimum green illumination (~13 kW/m^2), and *C* with the minimum blue illumination (~7 kW/m^2). Each picture is an average of 64 video frames (at 30 frames per second) from the ISIT camera. A computer-controlled shutter was used to minimize the specimen exposure. Time between pictures, with no illumination, 30 s. Every effort was made to keep the illumination to a minimum during selection and focusing, but in *C*, *1–6*, the microtubules are probably starting to break up by the time the first picture is taken. Bar, 10 μm.

at later times up to 30 min after dissolution, but no regrowth of MTs was detected. However, when fluorescent MTs were mixed with taxol-stabilized PC tubulin MTs, only some of the MTs dissolved, but these dissolved completely. MTs made from PC tubulin were unaffected by our conditions of illumination, so we assume that the MTs which dissolved from the mixture were the fluorescent ones. We conclude that the photobleached fluorescent tubulin will not disassemble existing MTs stabilized with taxol, though the data of Leslie et al. (1984) imply that unpolymerized, photodamaged subunits act as a strong poison to the assembly of new MTs. In another experiment, taxol-stabilized PC tubulin MTs at a concentration of 1 mg/ml were mixed with fluorescently labeled BSA (Molecular Probes Inc., Junction City, OR) at 1 mg/ml. No dissolution of the MTs was seen over 15 min of illumination. Thus, photobleaching of fluorescent groups on molecules that are not bound to the MTs will not promote disassembly of the MTs.

The Effects of Changing the f-to-p Ratio of the MTs. NHS-FTb was mixed with PC tubulin before assembly in 10 μM taxol, in order to change the f-to-p ratio of the assembled MTs. If the MTs have a lower f-to-p ratio they take longer to disappear (Fig. 4 *D*). NHS-FTb MTs with an f-to-p ratio of 0.25 dissolve in 120 s, as opposed to 40 s for similar MTs with an f-to-p ratio of 0.5 (Fig. 4 *C*). At low f-to-p ratios, individual breaks can be seen as they occur in the MTs. Fig. 5 shows the formation of one such break. The MT appears to bend under random thermal motion and then to break in two. All the MTs in the field appeared to break into successively shorter lengths in a random fashion, until they fell below the resolution of the DIC microscope. No ATP or GTP was included in the PME buffer, so the break up of the MTs does not appear to require a biological energy source.

Effects of Quenching Free Radical Reactions. Addition of 4 mM ascorbic acid completely prevented photodissolution of the MTs and also greatly reduced the photobleaching of the fluorescent tubulin. This implies that both the photobleaching and the photodissolution of the MTs occur by a free-radical mechanism of some sort. This is consistent with the previously published data on the photobleaching of DTAF-tubulin (Leslie et al., 1984).

An Hypothesis about Microtubule Photolability

These observations lead us to suggest that irradiation of fluorescent MTs induces photobleaching of the fluorescent subunits, which in turn produces structural damage that weakens the MTs. We suppose that after a sufficient number of tubulin subunits in one area have been damaged, the MTs break under the action of forces imposed by random thermal motion. After a sufficient number of breaks have occurred, the MTs disappear below the resolution limit of the DIC microscope and thus "dissolve." We call this behavior photodissolution or photolability. A quantitative model for the rate of photodissolution is given in the appendix.

Analysis of Microtubule Photodissolution In Vitro Using Laser Irradiation

The time taken for an MT to dissolve under irradiation provides a ready measure of the rate of photodissolution and can be used to assess the effects of different experimental conditions on the phenomenon. We have used DIC observation in green light, combined with epiillumination by blue argon laser light to measure the time to dissolution for NHS-FTb MTs under a variety of conditions, using laser irradiation intensities varying from 1 to 280 MW/m^2. This intensity range was chosen to give short times to dissolution under the conditions of our in vitro assay. It is intermediate between the intensity ranges commonly used for epifluorescent observation (3–700 kW/m^2) and laser photobleaching (up to 500 MW/m^2). In general the MTs were assembled in PME buffer supplemented with 10 μM taxol and 5% glycerol, and the laser irradiation was continued until the MTs had completely disappeared. This protocol simplified the analysis of the results. The effects of shorter illumination times and the effects of MAPs instead of taxol are presented later in this paper.

Fig. 6 shows the variation of the time until MT dissolution

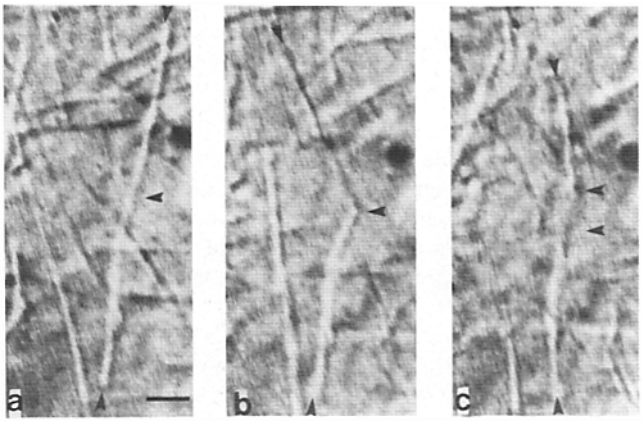

Figure 5. DIC images of a tube breaking. Succinimidyl-fluorescein MTs at an f-to-p ratio of 0.25 were illuminated with blue light, as in Fig. 4 *D*. At this f-to-p ratio the microtubules break up sufficiently slowly that individual breaks can be seen as they occur. One microtubule (*arrowheads*) can be seen to kink into a V shape and then break. Time between pictures is ~2 s. Bar, 5 μm.

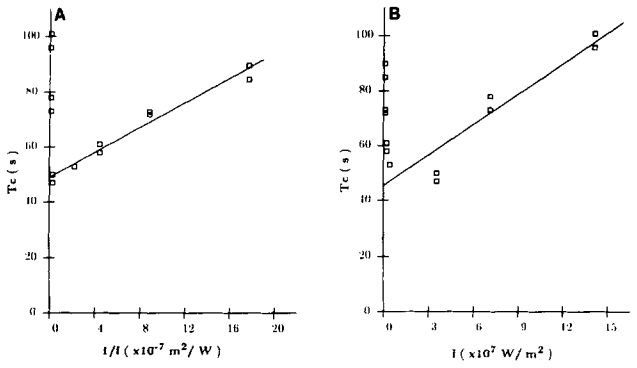

Figure 6. Plots of dissolution time against light intensity. Succinimidyl-fluorescein MTs were prepared at 2 mg/ml in PME + 5% glycerol at an f-to-p ratio of 0.5 and observed at 26°C (i.e., standard conditions). The time to dissolution (T_c) is plotted against the reciprocal of illumination intensity ($1/I$) in *A* and against illumination intensity in *B*. The same data are plotted in both graphs and in each case one part of the data fits well to a straight line. Note that at high intensities T_c increases with increasing I, while at low intensities T_c decreases with increasing I.

(T_c) with the intensity of the light used to irradiate them (I). The figure shows that T_c decreases with increasing light intensity up to a certain level and then increases with further increases in light intensity. Fig. 6 *B* shows that T_c is approximately linear with I at high intensities, and Fig. 6 *A* shows that T_c is linear with $1/I$ at low intensities. For the sake of clarity we will deal with the low and high intensity regimens separately below. It is interesting to note, however, that the linearity of T_c with $1/I$ at low intensities implies that an MT must be exposed to a certain amount of energy before it will break up completely (~2 megajoules [MJ]/m^2 under these conditions). Also, according to the least-squares fit straight line, the MTs would still take a certain amount of time to disappear even if this energy were delivered at infinite intensity ($1/I = 0$). This observation is consistent with the mechanism for photodissolution proposed above, since even if all the fluorescent subunits in the MT were bleached instantly, the MT would still take a certain amount of time to break up under thermal motion.

Low Light Levels, Constant Illumination. To characterize the MT photolability more fully, the T_c of taxol-stabilized fluorescent MTs was determined under a variety of conditions. Fig. 7, *A–C* shows graphs of the times taken for MTs to disappear, plotted against the reciprocal of the laser irradiation intensity under various conditions. These data show that the MTs disappear under all the conditions investigated and that the effect is approximately linear with the reciprocal of irradiating intensity. In these graphs, the intercepts of the lines (the times for dissolution extrapolated to infinite intensity) indicate the time required for the MTs to break up after complete photobleaching, and thus give information about the structural stability of the bleached MTs. The slopes of the lines indicate the rate of photodamage in response to irradiation (see Appendix for a more complete discussion). Fig. 7 *A* shows a plot of the variation of dissolution time with observation temperature. The slopes of the lines are approximately constant, but the intercepts decrease rapidly with increasing temperature. This behavior is consistent with our proposition that the mechanism of photodamage is largely independent of temperature, while the rate of break-up of an MT with a given amount of structural damage increases with thermal energy. Similarly Fig. 7 *B* shows that the intercept, but not the slope of the line, increases with glycerol concentration. This observation is readily explained by the assumption that an increasing concentration of glycerol will increase the viscosity of the solution and hence decrease both the agitation of the MTs and the rate of MT break-up for a given degree of photodamage. While temperature and glycerol concentration also have effects on microtubule stability in their own right, the MTs studied here are stabilized with 10 μM taxol, so we believe that these effects are not likely to be significant under the conditions used.

Our hypothesis predicts longer irradiation times for photodissolution of MTs with lower f-to-p ratios. Fig. 7 *C* shows that decreasing the f-to-p ratio of the tubulin by diluting the NHS-FTb with PC-Tb before assembly of the MTs increases both the slope and intercept of the line. Since individual fluorophores will have a constant probability of photobleaching for a given light level, a MT with low f-to-p ratio will acquire fewer weak spots per unit length after a given irradiation than one with a high f-to-p ratio (see Appendix). Our hypothesis therefore predicts longer irradiation times for photodissolution at lower f-to-p ratios, as observed. The data also show that the NHS-FTb will copolymerize with PC-tubulin.

High Light Levels, Constant Illumination. The above results are from data which were collected at light intensities of <5 MW/m^2. In general, epifluorescent images are collected under illumination from an arc light, which in our system ranged in intensity from 7 to 300 kW/m^2, while the photobleaching marks are made with a focused laser beam at intensities of up to 500 MW/m^2. We were therefore in-

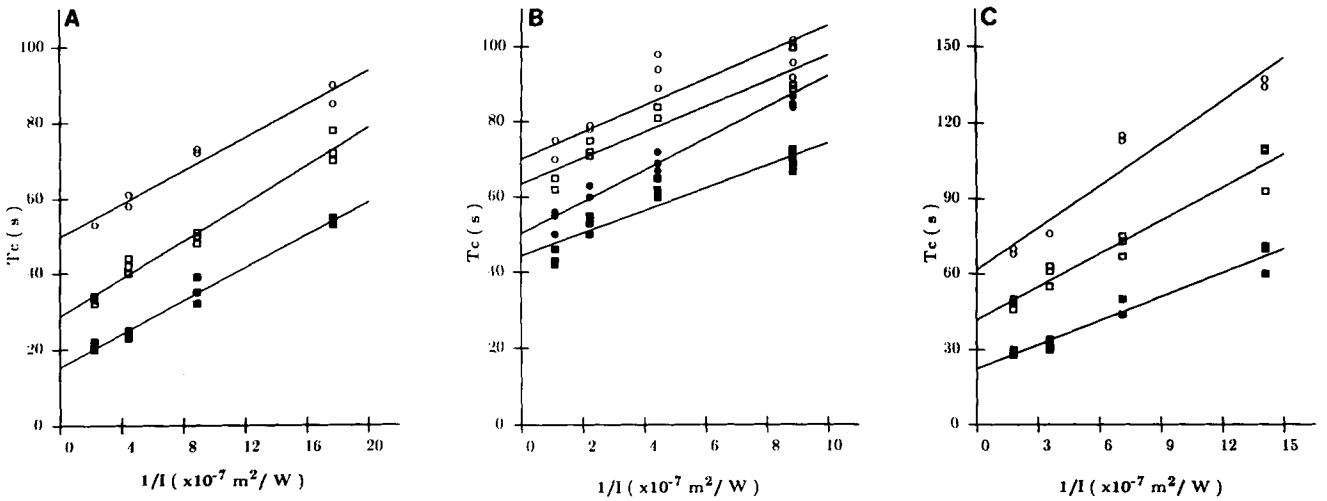

Figure 7. Plots of dissolution time at low light intensity. Succinimidyl-fluorescein MTs were prepared under standard conditions (i.e., at 2 mg/ml in PME + 5% glycerol and an f-to-p ratio of 0.5) and observed at 26°C unless otherwise stated. T_c is plotted against the reciprocal of illumination intensity. (*A*) Variation with observation temperature. (○, □, and ■) 26, 31, and 35°C, respectively. (*B*) Variation with glycerol concentration. (○, □, ●, and ■) 20, 10, 5, and 0% glycerol, respectively. (*C*) Variation with f-to-p ratio. (○, □, and ■) 0.125, 0.25, and 0.5 M f-to-p ratio, respectively. At a given light intensity, T_c decreases with increasing temperature and f-to-p ratio, and increases with increasing glycerol concentration. Note that none of these conditions affect the slope of the lines very much, indicating that they do not affect the mechanism of photodamage. However, they all affect the intercepts of the lines, indicating that they affect the rates of break-up of the damaged tubes. This is as one might expect from our proposed mechanism.

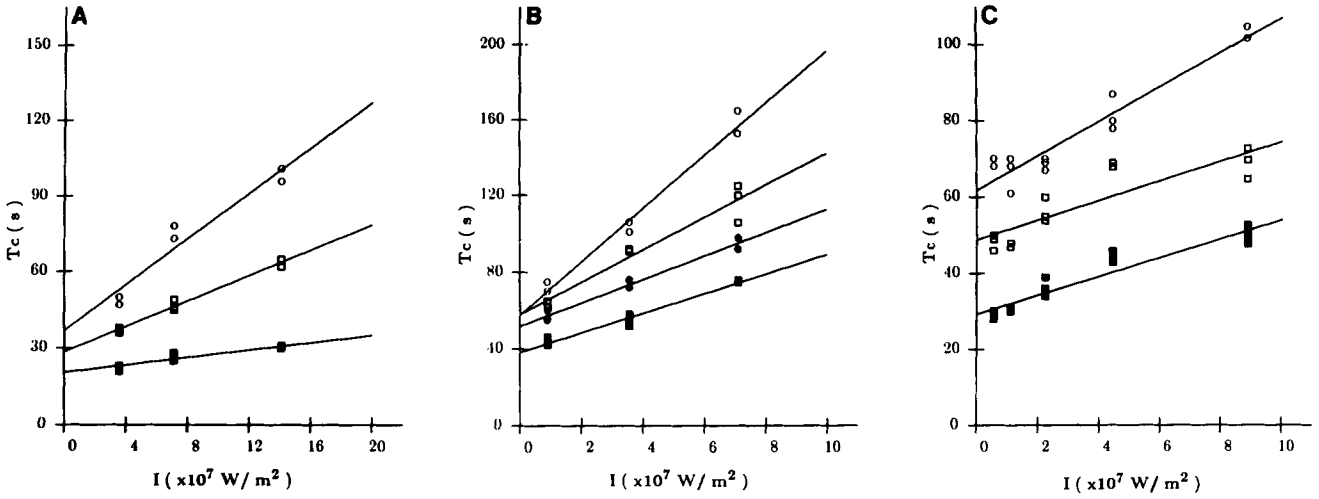

Figure 8. Plots of dissolution time at high light intensity. Succinimidyl-fluorescein MTs were prepared as in Fig. 7. T_c is plotted against illumination intensity. (*A*) Variation with observation temperature. (○, □, and ■) 26, 31, and 35°C, respectively. (*B*) Variation with glycerol concentration. (○, □, ●, and ■) 20, 10, 5, and 0% glycerol, respectively. (*C*) Variation with f-to-p ratio. (○, □, and ■) 0.125, 0.25, and 0.5 M f-to-p ratio, respectively. All the data fit well to straight lines calculated by linear regression. Note that the intercepts of the lines are close to those of the equivalent curves in Fig. 7 though calculated from different data.

terested to see if the same effect of photolability occurred at the very high light intensities usually used to produce photobleaching marks on fluorescent polymers in living cells. We found that they did, but with an added complication. Fig. 8, *A–C*, shows that at high light levels (>5 MW/m²) the MTs dissolved more slowly, not more quickly, with increasing light intensity. The times for dissolution at intensities >5 MW/m² increased linearly with intensity, rather than with the reciprocal of intensity. This implies that in addition to the photobleaching effect described above there is a second effect, which is important at high power densities but negligible at low ones and which complicates the photodissolution behavior. We assume that this effect either photobleaches the fluorescent moieties without weakening the MTs as much as photobleaching at low intensity does, or stabilizes the MTs against dissolution by the photodamaged subunits.

Fig. 8 shows that the rate of photodissolution at high intensities is affected by the same factors that influence it at low intensity. The data in this intensity range are more difficult to interpret, however, since the slopes of the lines as well as the intercepts are now effected by the specimen conditions. A more complete explanation of this is given in the Appendix. As before, however, increased temperature (Fig. 8 *A*) and increased f-to-p ratio (Fig. 8 *C*) are seen to decrease the time to dissolution for a given light intensity, while increasing glycerol concentration increases it (Fig. 8 *B*). Under all these conditions the T_c increases with light intensity.

We have explored some of the possible mechanisms for the decreased rate of MT photodissolution seen at high irradiation intensities. Calculations indicate that even our highest power density (~500 MW/m²) is four orders of magnitude too low to give photon-doubling events, so such effects are unlikely to be significant (Peters, K., personal communication). One might imagine that high intensity irradiation would promote extensive protein cross-linking, and thereby stabilize the MTs, but SDS-PAGE gels of specimens bleached at high and low light intensities show no marked differences. Both specimens show molecular weight species higher than tubulin, which probably correspond to cross-linked proteins, but the photostabilized preparations are not noticeably more cross-linked than those bleached at low light intensity (data not shown; see Leslie et al., 1984). A plausible explanation for the effect, in view of the very high energy densities at which it is seen, is that the photostabilization is due to local heating of the MTs by the laser beam.

We have tested the idea of a thermal mechanism for photostabilization by using a coverslip shadowed lightly with gold. Since the evaporated gold appeared blue in transmission it did not absorb very much energy from the blue laser light, but greatly increased the thermal conductivity of the specimen immediately adjacent to the coated coverslip. At low intensities, the rate of photodissolution was hardly changed (Fig. 9 *A*), but at high intensities the rate of stabilization was reduced by ~13-fold (Fig. 9 *B*). MTs bleached in the medium away from the gold-shadowed coverslip, on the other hand, showed normal behavior in both photolability and photostabilization. These results are consistent with our proposal that photostabilization is a thermal effect that depends on a local temperature rise.

Local heating might be expected to stabilize MTs against depolymerizing agents such as cold or 10 mM calcium. However, under all depolymerizing conditions we tried, the irradiated MTs broke up faster than unbleached MTs. Under our conditions of photobleaching, then, high intensity irradiation of fluorescent MTs does not actually stabilize the polymers relative to unbleached MTs; it simply modulates the photodissolution effect.

Short Illuminations. The results described so far were obtained by irradiating the specimen at constant intensity until the MTs had dissolved. This was done to minimize the number of variables in the experiments, but the conditions do not correspond well to those used for experiments on fluorescent MTs in vivo. Fig. 10 shows the dependence of time for MT dissolution on irradiation time at two intensities. The two light intensities used, 2.2 MW/m² and 71 MW/m², differed by a factor of 30 but gave approximately

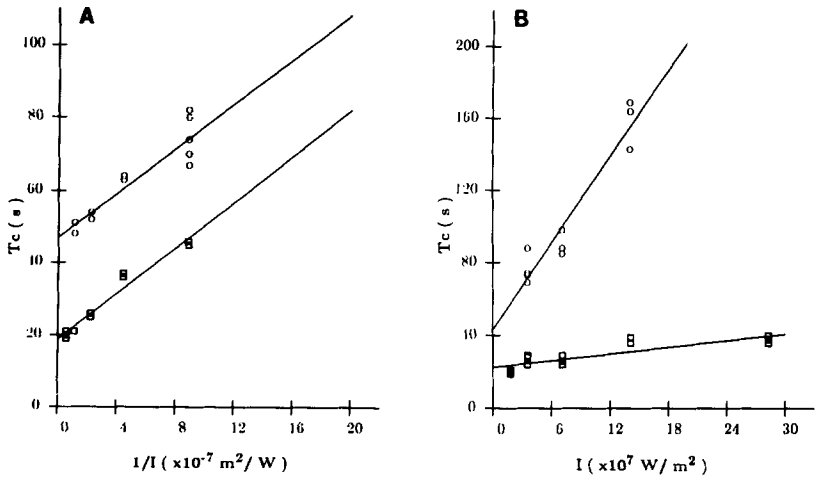

Figure 9. Gold-shadowed coverslip. Microtubules were compared under standard conditions near the glass coverslip (○) or near a coverslip shadowed with gold (□). The gold shadow has little effect on the rate of photodissolution at low intensity (*A*), but reduces the rate of photostabilization by 13-fold at high intensity (*B*).

the same T_cs under conditions of continuous illumination, because the fluorescent MTs exhibited photostabilization upon irradiation at 71 MW/m² but not at 2.2 MW/m². As the time of irradiation (T_i) was increased, the T_c decreased for MTs irradiated at either intensity. For MTs irradiated at 71 MW/m², T_c did not change rapidly if T_i was longer than ~2 s, whereas for MTs irradiated at 2.2 MW/m² T_c became approximately constant only for T_i >20 s. By observing the MTs with fluorescence optics, we observed that the tubulin fluorescence was heavily bleached after 2 s of irradiation at the higher intensity (data not shown), and so one may infer that most of the photobleaching important for photodissolution occurred within the first 2 s of irradiation. Similarly, at low light intensities most photobleaching has probably occurred within ~20 s. At times shorter than these, the MTs are presumably only partially photobleached and therefore break up at slower rates. We were unable to generate a simple mathematical model for this behavior. It is interesting to note, however, that the total energy required to promote complete dissolution of the MTs at low light levels (2 MJ/m² at this f-to-p ratio) is much less than the energy required to give near-total photobleaching of the fluorescent tubulin at these f-to-p ratios (~140 MJ/m², based on data from this section). Thus, complete photobleaching is not required to give MT dissolution at these f-to-p ratios. This result is confirmed by the in vivo experiments (Fig. 3), which show that the fluorescent MT arrays in cells are apparently dissolved before all the MT fluorescence is bleached.

Wavelength Dependence. To investigate the wavelength dependence of photodissolution, we selected four wavelengths from the argon-ion laser emission spectrum, and measured the intensity dependence of dissolution of NHS-FTb MTs at each wavelength (476.5 nm, 488.0 nm, 496.5 nm, and 514.5 nm). Both photodissolution and photostabilization of the fluorescent MTs depended on the wavelength of irradiation. The rates of both photodissolution and photostabilization were proportional to the absorbance of the fluorescent tubulin at that wavelength. The slowest photodissolution and least effective photostabilization occurred at the wavelength at which the fluorophore absorbed least strongly (514.5 nm), while all three strongly absorbed wavelengths gave rapid photobleaching and strong photostabilization.

Other Factors that Effect the Rate of Photodissolution. When the MTs were heavily bundled or stuck to the glass coverslip, the observed time for dissolution increased. If polylysine was used to stick the MTs down, they did not dissolve at all. On the other hand, if a TV camera with lower resolution was used to observe the MTs during irradiation, the time for apparent dissolution decreased. Presumably the judgement of the time for dissolution of the MTs depends on the contrast of the DIC optics and on the resolution of the video system. These factors were therefore carefully controlled during collection of our data.

If the MTs were assembled in PME buffer in the presence of 0.2 mg/ml MAPs + 1 mM GTP rather than 10 μM taxol, photolability was again observed, but the rate for photodissolution was now much faster (data not shown). This is probably because taxol stabilizes MTs over their entire lengths, while once a MAP-stabilized MT breaks, one half of it is able to disassemble rapidly from its plus end, thereby increasing the overall rate of dissolution (cf., Horio and Hotani, 1986). The slope of the line relating T_c to $1/I$ does not change, however, indicating that the mechanism of photodamage has not been altered.

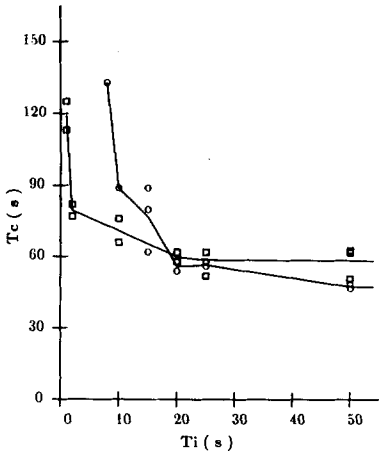

Figure 10. Plots of dissolution time for short illuminations. Microtubules were irradiated for various times (T_i) at 2.2 MW/m² (○) or 71 MW/m² (□) with blue laser light and then observed under green, nondamaging light to measure the T_c. Both light intensities give approximately the same T_c at long T_i, but have different effects at low T_c.

Addition of 4 mM dithiothreitol to NHS-FTb MTs, which will act to reduce disulphide bonds, increased the rate of photodissolution of taxol-stabilized MTs, for reasons that are not clear.

The photodissolution effect was also seen with MTs made from DTAF-tubulin with an f-to-p ratio of 0.1 (data not shown). The rate of photodissolution for these MTs was approximately the same as that seen with MTs assembled from NHS-FTb. Since the DTAF MTs had one-fifth the f-to-p ratio. the photodissolution effect must be stronger in DTAF-tubulin than in NHS-FTb. The extent of photostabilization was reduced, however, as expected for an MT with a lower number of fluorophores per unit length and hence less capacity to transduce light energy to heat.

As stated above, the addition of 4 mM ascorbic acid blocked photobleaching and stopped photodissolution at low intensities. Interestingly, at high light intensities the MTs could be seen in epifluorescence to be somewhat bleached, but they did not dissolve. This implies either that the ascorbic acid decouples photobleaching from photodissolution, or that at high intensities the MTs still undergo photostabilization in the presence of ascorbic acid, and thus do not break up on photobleaching.

We also examined the behavior of MTs made from an NHS-RTb kindly provided by Dr. T. Mitchison, which was prepared using a somewhat different protocol (Kellogg et al., 1988). Mitchison's NHS-RTb had a higher f-to-p ratio than our NHS-RTb, and was thought to be ~100% labeled. When this tubulin derivative was incubated with 10 μM taxol it produced MTs that appeared somewhat aberrant in the DIC microscope, since they always assembled as short fragments that did not form longer MTs after extended incubation. However, these MT fragments displayed the same photolability as MTs prepared from our own NHS-RTb. The rate of photodissolution was in fact considerably faster than with our NHS-RTb (60 s as opposed to 300 s under the same conditions as Fig. 4), probably because of the higher f-to-p ratio of this preparation. Dilution of the labeled tubulin with unlabeled tubulin reduced its rate of photodissolution.

At low intensities, the NHS-RTbs display the same relationship between T_c and light intensity as the NHS-FTb, but with lower rates. We have not been able to measure the time dependence of dissolution at high light intensities, because our laser does not emit light at the appropriate wavelengths.

Discussion

We have shown that a variety of amine-reactive fluorescent molecules may be used to make analogues of tubulin that show good assembly dynamics in vitro and which will incorporate into the cytoskeleton of living cells to give excellent high brightness images. Other workers have made similar fluorescent analogues (Gorbsky et al., 1988; Kellogg et al., 1988), but this paper includes the first characterization of their assembly properties and the sensitivity of the resulting MTs to light. Polymers of all the analogues tested appear to lose their structural integrity upon irradiation with light at the intensities and wavelengths used for fluorescence microscopy. We call this effect photodissolution. Fluorescent MTs appear to dissolve before they lose all their fluorescence. We have investigated this phenomenon using a DIC-based in vitro assay to measure the T_c of the MTs. We chose to use this assay, rather than more conventional methods such as turbidometry or viscometry, because it gave high time resolution and was applicable to small samples. Most importantly, the microscopic assay enabled us to irradiate well-controlled samples with light intensities comparable to those used for FRAP studies in vivo. The irradiation of even a 1-mm^3 sample at 200 MW/m^2 would have required a 200-W continuous wave laser, a device that was well beyond our reach. We have developed a conceptual model that quantitatively explains the data gathered. The model may not be physically correct, and we present it mainly to provide a conceptual frame-work within which one may consider the data. However, the model is plausible, reasonably simple, and is the only one we have found that fits all the available data. We postulate that photobleaching of the fluorescent subunits at medium to low power densities (up to 5 MW/m^2 under the conditions of our in vitro assay) leads to sufficient weakening of the MTs that they will break up under stresses as small as those applied by random thermal motion. We can propose no specific mechanism for the process of photodamage, except that it probably occurs by a pathway that involves free radicals.

We have also shown that the photodissolution of fluorescent MTs is modulated by a second effect which we have termed photostabilization. We tentatively suggest that this photostabilization may be due to local heating of the MTs at high light intensities. The effect requires more complete characterization than we have been able to provide here, but we think that an explanation based on local heating of the MTs is reasonable, in view of the very high power densities at which it is observed. To appreciate the magnitude of these energies, it is instructive to realize that an energy density of 10 MW/m^2 is ~1,000-fold that seen by a chicken in a microwave oven! Thus, while our data indicate that temperature increases between 26 and 36°C increase the rate of MT dissolution, probably due to increased thermal motion, higher temperatures would be expected to denature the tubulin. Fluorescein attached to protein at pH 6.9 has a fluorescence quantum efficiency of ~0.5 (Mathies and Stryer, 1986), so a significant fraction of the incident energy from the laser beam may be converted to heat by the fluorophore. This could raise the local temperature of the tubulin and convert it into a form that was less able to break down upon photobleaching. At an intensity of 70 MW/m^2 a solution of NHS-FTb MTs at 2 mg/ml and an f-to-p ratio of 0.5 would, in the absence of heat dissipation, experience a temperature jump of 40°C before photobleaching. Such a temperature increase would probably be more than sufficient to damage the tubulin. This estimated temperature jump is much greater than the 0.03°C calculated by Axelrod for fluorescent probes on a membrane (Axelrod, 1977), because we assume that light is being converted to heat throughout the volume of the MT suspension and because we are taking the limiting case of infinite power, where no heat would be dissipated from the irradiated volume. However, smaller temperature jumps would still be sufficient to damage the MTs, which is probably why the photostabilization effect appears to be proportional to power density.

The photostabilization effect only occurs at very high power densities, under the conditions of our in vitro assay, and hence may be negligible for many FRAP experiments. However, we feel that the effect deserves further study since, if

it is mediated by local heating as proposed above, it could have significant effects in vivo on other proteins near the MTs in the irradiated region. Also, the rhodamine tubulins should show the effect more dramatically than the fluorescein tubulins, because both the rate of photobleaching and the quantum efficiency of the rhodamines are lower (Johnson and Garland, 1982).

Several previous studies have examined the properties of fluorescent tubulins, so one may ask why the photolability described here was not recognized sooner. A number of factors probably contributed to this situation. The DTAF-tubulin of Leslie et al. (1984) was reported to have an f-to-p ratio of ~1.0, but we suggest that this was an overestimate, because of dye in the preparation that was not covalently bound to the tubulin. We have found that free DTAF runs in front of the Coomassie Blue dye front on SDS gels and is only weakly fluorescent in this environment (see Fig. 1). Thus it probably escaped detection in the previous experiments. The f-to-p ratio of the DTAF-tubulin, which we have made, is ~0.1 after removal of the unbound dye. For a given amount of tubulin analogue injected into a cell, the DTAF-tubulin preparation would display a lower rate of photodissolution compared to a more fully derivatized analogue and would also show a lower fluorescence brightness for the observation of the photodissolution effect. Any free dye present would also increase the background fluorescence in the cell, making observation still more difficult. Injection of PtK1 cells with our NHS-FTb analogue gives significantly brighter images, with less background fluorescence, than does injection with the DTAF-tubulin, making the photodissolution effect easier to observe (Fig. 3). Furthermore, the photodissolution that occurs during specimen selection and focusing may have degraded the DTAF-tubulin image to the point where further degradation of the image during observation was not obvious. The in vitro experiments of Leslie et al. (1984) do in fact contain some data which are suggestive of MT photodissolution (e.g., their Figs. 7 and 8), but other explanations were available to them at the time and the effect was judged to be acceptable, since the protein was thought to be 100% fluoresceinated.

Experiments were done in previous studies to check the ultrastructural morphology of the MTs after photobleaching, but the specimens were prepared for EM immediately after photobleaching (Leslie et al., 1984; Saxton et al., 1984). Our results show that some time is required before the dissolution effects of irradiation are detectable. Unfortunately, video-enhanced DIC microscopy was not available for the real-time observation of individual MTs at that time.

Controls on DTAF-tubulin injected into sea urchin eggs (Salmon et al., 1984*a*), which used polarization optics to monitor the birefringence of the spindle, failed to show any change in birefringence after laser photobleaching. On the other hand, FRAP studies of injected mitotic PtK1 cells have indicated that the spindle shrinks somewhat upon extensive, low intensity illumination (Stemple et al., 1988). The differences in these results might well result from the large reservoir of unlabeled and unassembled tubulin which is available to replace the fluorescent tubulin as it is photodamaged in the sea urchin egg, but not in the mammalian cell. Further, photobleaching at high intensity appears to do less net damage than prolonged illumination at low intensity.

The most important question about the effects described here is their impact on the data generated by experiments using FRAP. Our in vitro experiments show that a wide variety of variables affect the behavior of fluorescent MTs on irradiation, and that there are at least two effects to be considered: photodissolution and photostabilization. The conditions under which the fluorescent tubulin analogues are used in vivo are also considerably different from those of our in vitro assay: (*a*) the f-to-p ratio of the MTs is lower, thanks to the dilution of the fluorescent protein by endogenous tubulin; (*b*) the irradiation intensities used for observation are lower (7–300 kW/m^2 as opposed to 1 to 5 MW/m^2); (*c*) the irradiation times during observation are shorter; (*d*) the cellular viscosity is probably higher; and (*e*) a variety of free radical scavengers such as glutathione are present in the cytoplasm. All these factors will tend to mitigate the effects of photodissolution. On the other hand, the optimum physiological temperature for many cells is higher than that at which the in vitro experiments were done (26°C) and MAPs are present rather than taxol. These effects will increase the rate of photodissolution. Also, the high light intensities used for photobleaching and the presence of free radical scavengers will make the effects of heating more severe, since the fluorescent groups will last longer and therefore transduce more heat before they are photobleached. Furthermore, there are probably other forces, such as tension or flexing, acting on cytoskeletal MTs in addition to Brownian motion, which would tend to make the MTs break up more quickly.

It must also be noted that our criterion for dissolution of the MTs in vitro was very severe. The photodissolution effect could have important consequences on the observed rates of MT turnover, even if all the MTs were not broken down into lengths below the resolution of the DIC microscope. Most significantly, the effect was first seen in vivo, before its existence was even suspected. Fig. 3 shows that the phenomenon can be important under conditions typical of those used in FRAP studies of tubulin. The apparent MT T_c in vivo using low light level epifluorescence and discontinuous illumination, were comparable to those observed with more intense continuous illumination in vitro. We conclude that photodissolution of fluorescent MTs is likely to have been going on during most of the experiments on the dynamics of fluorescent tubulin so far reported, both from this and from other laboratories.

Nonetheless, it is probable that many of the published deductions from FRAP studies of DTAF-tubulin are still correct. For instance, it is likely that the relative rates of incorporation and turnover of tubulin in mitotic and interphase cells really are very different (for sea urchin eggs see Wadsworth and Sloboda, 1983; Salmon et al., 1984*a*; and for mammalian cells see Saxton et al., 1984; Wadsworth and Salmon, 1986; Mitchison et al., 1986; Schulze and Kirschner, 1986), both because the rates estimated from FRAP studies differ so greatly (by more than a factor of ten) and, more importantly, because similar results have been obtained with several independent methods (e.g., Salmon et al., 1984*b*; Cassimeris et al., 1986). The rates measured for MT turnover in vivo by FRAP, however, are probably a compound of the true rates and the rates of MT disassembly and repair after breakage of the MTs due to photodamage. How accurate an estimate of the true turnover rates these are remains to be seen.

At a somewhat more problematical level, the data col-

lected by several groups on the movement of mitotic spindle MTs must now be interpreted with some care. Such interpretation requires an accurate knowledge of the behavior of the partially photobleached bundles of fluorescent MTs, which are probably under load in the spindle. This knowledge is not available at the present time. Our observations on the photodissolution of fluorescent MTs may contribute to an explanation of the discrepancies between data on the movements of areas of reduced birefringence (Forer, 1965) and of fluorescent photobleaching marks in mitotic spindle MTs (Saxton and McIntosh, 1987; Gorbsky et al., 1987, 1988). Our observations may also explain the discrepancies between the FRAP data that show no enhanced stability of the kinetochore MTs (McIntosh and Vigers, 1987) and the results of drug and cold block studies that do (e.g., Brinkley et al., 1975). Similarly, the reports of dynamic instability observed in the borders of living cells injected with fluorescent analogues (Sammak and Borisy, 1988) must be viewed with some caution. It is possible that the MTs are either induced to display partial dynamic instability or prevented from complete disassembly by the photodissolution and photostabilization effects described here. Sophisticated controls will be required to exclude the possibility of light induced artifacts.

One may ask what can be done to minimize the impact of these effects on FRAP experiments. One possibility is that a search for better fluorescent tags will yield tubulin analogues with dramatically different properties from those described here. However, it may not be coincidental that all the fluorescent analogues of tubulin that have been shown to have good assembly properties are made with amine-selective reagents (Keith et al., 1981; this paper) and that all the analogues we have tested display the photolabile behavior. It is also interesting to note that two fluorescent analogues of actin have recently been shown to display a behavior similar to the photodissolution described here (Simon et al., 1988). No photostabilization has yet been observed with actin, but lower power densities (<0.5 MW/m^2) were used in these studies. This similarity of behavior may indicate that photodissolution of fluorescent polymers is a more widespread problem than one might expect. If better fluorescent analogues cannot be made, on the other hand, it is possible that the photodissolution effect could be used to advantage, since the fluorescent tubulin could be used as a "Trojan Horse": it could be introduced into the cell, and then all the MTs in a specified region of the cell (e.g., around the centrosome or kinetochore) could be dissolved on demand. Whether this approach has practical applications remains to be seen.

Apart from the production of better analogues, it is possible that the photodissolution effect could be reduced to a negligible level by careful limiting of the light intensities used for observation, particularly with the rhodamine analogues. However, it would be difficult to prove that one had reached this limiting situation, since as the light intensity is lowered the errors in the observations will increase and the photodissolution will be more difficult to detect. Furthermore, it is not clear how one can make photobleached marks in fluorescently labeled structures without introducing the possibility of photodissolution or photostabilization. A more promising approach might be to use cells with very large reservoirs of unlabeled tubulin, such as sea urchin eggs or Drosophila embryos (e. g., Kellogg et al., 1988). In this way, the photodamaged subunits could be diluted into an effectively infinite pool, thus mitigating any effects from photodamaged subunits or from a change in the net tubulin pool. This approach, however, would not alter the effects of photodissolution on the apparent tubulin turnover rates.

Until these questions are resolved, the problems of photodissolution and photostabilization must seriously limit the usefulness of fluorescent analogues for the study of MT dynamics, particularly with FRAP methods. It is difficult to say precisely how these properties will affect MTs in vivo, since a large number of factors have been shown to modulate the rate of break up of the MTs in vitro and since we do not yet have sufficient data on the internal conditions of the cell to be able to decide which factors are important in vivo. Until this problem is resolved, FRAP data on tubulin dynamics must be interpreted with the greatest care.

We thank Dr. T. Mitchison for sending us a sample of his NHS-RTb, Dr. D. Lancing Taylor for sending us a preprint of the paper from his lab on the photodestruction of fluorescently labeled actin, and Dr. David Agard for telling us about his work on the effects of lens aberrations. We also thank Tanya Falbel for making the initial observations of photodissolution in vivo that prompted the work reported in this paper.

This work was supported by grant GM-33787 from the National Institutes of Health to J. R. McIntosh. Guy Vigers is supported by a North Atlantic Treaty Organization postdoctoral fellowship. Martine Coue is supported by the Centre Nationale de la Recherche Scientifique.

Received for publication 18 April 1988, and in revised form 18 May 1988.

Appendix

A Model for the Photobleaching of Fluorescent Microtubules

Low Intensity, Constant Illumination. Suppose that a microtubule has F fluorescent subunits per unit length at time t. Then the rate of production of photobleached subunits is given by

$$\frac{dB}{dt} = F\alpha I,$$

where B is the number of photobleached subunits per unit length, I is the incident light intensity, and α is the probability of photobleaching per fluorescent moiety per incident photon. F is the number of fluorescent subunits per unit length at time t, and therefore contains the prior photobleaching history of the microtubules. Thus, the number of bleached subunits per unit length B at time t is given by

$$B = F_0 (1 - e^{-I\alpha t}),$$

where F_0 is the initial number of fluorescent subunits per unit length. Now, assuming that the rate of production of breaks is proportional to the number of subunits that have bleached, then

$$\frac{dN}{dt} = \frac{B}{\gamma},$$

where N is the number of breaks per unit length and γ is a proportionality constant. We expect γ to be a function of the viscosity and temperature of the surrounding medium, the structural rigidity of the damaged subunits, etc. Therefore,

$$\frac{dN}{dt} = \frac{F_0(1 - e^{-I\alpha t})}{\gamma},$$

or

$$N = \frac{F_0}{\gamma}\left[t + \frac{e^{-I\alpha t}}{\alpha I}\right]_0^t.$$

If the tube disappears below the resolution of the light microscope when

$$N = N_c \text{ and } t = t_c,$$

then

$$\frac{N_c\gamma}{F_0} = t_c + \frac{(e^{-I\alpha t_c} - 1)}{\alpha I};$$

and if

$$e^{-I\alpha t_c} \ll 1,$$

then

$$t_c \approx \frac{N_c\gamma}{F_0} + \frac{1}{\alpha I}.$$

Therefore, a plot of time to dissolution (T_c) against $1/I$ should yield a straight line, with

$$\text{intercept} = \frac{N_c\gamma}{F_0} \text{ and slope} = \frac{1}{\alpha}.$$

However, this analysis is somewhat inadequate, since once a tube has broken it cannot break again at the same place. Therefore, a more accurate representation is given by

$$\frac{dN}{dt} = \frac{(B - N)}{\gamma}$$

or

$$N + \gamma\frac{dN}{dt} = F_0(1 - e^{-I\alpha t}).$$

This equation has the solution

$$N_c = F_0\left[1 - \frac{e^{-I\alpha t_c} - I\alpha\gamma e^{-t_c/\gamma}}{1 - I\alpha\gamma}\right].$$

At large I (small $1/I$) this simplifies to

$$N_c \approx F_0(1 - e^{-t_c/\gamma}),$$

and if

$$t_c/\gamma \ll 1$$

then (as above)

$$t_c \approx \frac{N_c\gamma}{F_0},$$

whereas for small I (large $1/I$)

$$N_c \approx F_0(1 - e^{-I\alpha t_c})$$

and

$$t_c = N_c/F_0\alpha I.$$

Therefore, a plot of T_c against $1/I$ should yield a straight line, with

$$\text{intercept} \approx \frac{N_c\gamma}{F_0} \text{ and slope} \approx \frac{N_c}{F_0\alpha}.$$

Thus the intercepts of the T_c against $1/I$ curves should be proportional to γ, which is related to the viscosity and temperature of the solution, as shown in Fig. 7, *A* and *B*. Similarly, both the slope and the intercept of the curves should be inversely proportional to the f-to-p ratio of the MTs. Fig. 7 *C* supports this interpretation. Furthermore, the slopes of the curves, but not the intercepts, should be inversely proportional to α, which represents the efficiency of photobleaching. Fig. 10 shows that α is large for wavelengths where the absorption of the fluorescent tubulin is high and small for wavelengths where the absorption is low, as expected.

High Intensity, Constant Illumination. If we assume that the unbleached fluorophores transduce the irradiating light into heat and thus stabilize the photobleached subunits against dissolution, to a degree that is proportional to the light intensity, and if we assume that all photobleaching and heating effects occur at times very short compared to T_c, then the number of photobleached subunits B is equal to the original number of fluorescent subunits:

$$B = F_0.$$

But now the number of photolabile subunits per unit length, L, is given by

$$L = Be^{-\delta I},$$

where δ is related to the rate of doing heat-induced damage. Then, if the total number of photolabile subunits is very much greater than the number of breaks required to make the MTs disappear, the number of breaks at time t is given by

$$N = \frac{Lt}{\gamma}.$$

Therefore,

$$N_c = \frac{F_0 t_c e^{-\delta I}}{\gamma}$$

and

$$t_c = \frac{N_c\gamma e^{\delta I}}{F_0};$$

and if

$$\delta I \ll 1,$$

then

$$t_c = N_c\frac{\gamma}{F_0}(1 + \delta I).$$

Therefore a plot of T_c against I should give a straight line with

$$\text{intercept} = \frac{N_c\gamma}{F_0} \text{ and slope} = \frac{N_c\delta}{F_0}.$$

Thus both the slopes and the intercepts of the T_c against I curves should be proportional to γ, which is related to the viscosity and temperature of the solution, and inversely proportional to the f-to-p ratio of the MTs, as shown in Fig. 8, *A-C*. Furthermore, the slopes of the curves, but not the intercepts, should be proportional to δ, which represents the efficiency of photoinduced heating. Fig. 10 shows that δ is large for wavelengths where the absorption of the fluorescent tubulin is high and small for wavelengths where the absorption is low, as expected. Note also that the intercept of the T_c/I curve should be the same as the intercept of the $T_c/(1/I)$ curve, as seen in all figures.

Furthermore, from the plot of T_c against $1/I$ in Fig. 6 *A* we get

$$\frac{N_c\gamma}{F_0} \approx 50 \text{ s and } \frac{N_c}{F_0\alpha} \approx 2.27 \times 10^7\ Jm^{-2},$$

and from the plot of T_c against I in Fig. 6 *B* we get

$$\frac{N_c\gamma}{F_0} \approx 45 \text{ s and } \frac{N_c\gamma\delta}{F_0} \approx 3.73 \times 10^{-7} \text{ s } W^{-1}\ m^2.$$

Now N_c and F_0 are hard to evaluate, since N_c is a function of the microscope imaging system and the effective value of F_0 is determined by the quaternary structure of the microtubule. Nonetheless, complete dissolution of microtubules has been observed using microtubules with an f-to-p ratio a factor of 10 lower than that of the microtubules in Fig. 6, so

$$F_0 \geq 10\ N_c.$$

Therefore,

$$1/\alpha \approx 2.27 \times 10^6\ Jm^{-2},$$
$$\delta \approx 8.3 \times 10^{-9}\ W^{-1}\ m^2,$$

and

$$\gamma \approx 500 \text{ s}.$$

Now if $I = 5$ MW/m^2 and $T_c = 50$ s, then

$$I\alpha t_c \approx 100 \text{ and } e^{-I\alpha t_c} \ll 1, \text{ as assumed},$$

$$\frac{t_c}{\gamma} \approx 0.1 \text{ and } \frac{t_c}{\gamma} \ll 1, \text{ as assumed},$$

and

$$\delta I \approx 4 \times 10^{-2} \text{ and } \delta I \ll 1, \text{ as assumed}.$$

Furthermore,

$$1/\alpha \approx 5.56 \times 10^{24} \text{ photons } m^{-2}$$

at 488 nm, or

$$1/\alpha \approx 1.7 \times 10^5 \text{ photons fluorescein}^{-1}$$

using the published capture cross-section for fluorescein of 3×10^{-20} m^2 (Mathies and Stryer, 1986). Therefore

$$\alpha \approx 6 \times 10^{-6} \text{ fluoresceins photon}^{-1}$$

which is within a factor of 5 of the published rate for fluorescein photobleaching of 2.7×10^{-5} photons fluorescein^{-1} (Mathies and Stryer, 1986).

References

Axelrod, D. 1977. Cell surface heating during fluorescence photobleaching recovery experiments. *Biophys. J.* 18:129–131.

Bradford, M. M. 1976. A rapid sensitive method for quantitation of microgram quantities of protein utilizing the principle of protein-dye binding. *Anal. Biochem.* 72:248–254.

Brinkley, B. R., and J. Cartwright, Jr. 1975. Cold labile and cold stable microtubules in the mitotic spindle of mammalian cells. *Ann. NY Acad. Sci.* 253:428–441.

Cassimeris, L. U., P. Wadsworth, and E. D. Salmon. 1986. Dynamics of microtubule depolymerization in monocytes. *J. Cell Biol.* 102:2023–2032.

Forer, A. 1964. Local reduction of spindle fiber birefringence in living Nephrotoma suturalis (Loew) spermatocytes induced by ultraviolet irradiation. *J. Cell Biol.* 25:95–117.

Gorbsky, G. J., P. J. Sammak, and G. G. Borisy. 1988. Microtubule dynamics and chromosome motion visualized in living anaphase cells. *J. Cell Biol.* 106:1185–1192.

Gorbsky, G. J., P. J. Sammak, and G. G. Borisy. 1987. Chromosomes move poleward in anaphase along stationary microtubules that coordinately disassemble from their kinetochore ends. *J. Cell Biol.* 104:9–18.

Horio, T., and H. Hotani. 1986. Visualisation of the dynamic instability of individual microtubules by dark-field microscopy. *Nature (Lond.).* 321:605–607.

Johnson, P., and P. B. Garland. 1982. Fluorescent triplet probes for measuring the rotational diffusion of membrane proteins. *Biochem. J.* 203:313–321.

Keith, C. H., J. R. Feramisco, and M. Shelanski. 1981. Direct visualisation of fluorescein-labeled microtubules in vitro and microinjected fibroblasts. *J. Cell Biol.* 88:234–240.

Kellogg, D. R., T. J. Mitchison, and B. M. Alberts. 1988. Behavior of microtubules and actin filaments in living Drosophila embryos. *Dev. Biol.* In press.

Laemmli, U. K. 1971. Cleavage of structural proteins during the assembly of the head of bacteriophage T4. *Nature (Lond.).* 227:680–685.

Leslie, R. J., W. M. Saxton, T. J. Mitchison, B. Neighbors, E. D. Salmon, and J. R. McIntosh. 1984. Assembly properties of fluorscein-labeled tubulin in vitro before and after fluorescence bleaching. *J. Cell Biol.* 99:2146–2156.

Mathies, R. A., and L. Stryer. 1986. Single-molecule fluorescence detection: a feasibility study using phycoerythrin. *In* Applications of Fluorescence Imaging in the Biomedical Sciences. D. L. Taylor, A. S. Waggoner, R. F. Murphy, F. Lanni, and R. R. Birge, editors. Alan R. Liss, Inc., New York. 129–140.

McIntosh, J. R., and G. P. A. Vigers. 1987. Microtubule dynamics in the mitotic spindle. *Proc. Electron Microscopy Soc. Amer.* 45:794–797.

Mitchison, T. J., L. Evans, E. Schulze, and M. Kirschner. 1986. Sites of assembly and disassembly in the mitotic spindle. *Cell.* 45:515–527.

Salmon, E. D., R. J. Leslie, W. M. Saxton, M. L. Karow, and J. R. McIntosh. 1984. Spindle microtubule dynamics in sea urchin embryos: analysis using a fluorescein-labeled tubulin and measurements of fluorescence redistribution after photobleaching. *J. Cell Biol.* 99:2165–2174.

Salmon, E. D., M. McKeel, and T. Hays. 1984. Rapid rate of tubulin dissociation from microtubules in the mitotic spindle in vivo measured by blocking polymerization with colchicine. *J. Cell Biol.* 99:1066–1075.

Sammak, P. J., and G. G. Borisy. 1988. Direct observation of microtubule dynamics in living cells. *Nature (Lond.).* 332:724–726.

Saxton, W. M., and J. R. McIntosh. 1987. Interzone microtubule behavior in late anaphase and telophase spindles. *J. Cell Biol.* 105:875–886.

Saxton, W. M., D. L. Stemple, R. J. Leslie, E. D. Salmon, M. Zavortink, and J. R. McIntosh. 1984. Tubulin dynamics in cultured mammalian cells. *J. Cell Biol.* 99:2175–2186.

Schulze, E., and M. Kirschner. 1986. Microtubule dynamics in interphase cells. *J. Cell Biol.* 102:1020–1031.

Simon, J. R., A. Gough, E. Urbanik, F. Wang, B. R. Ware, and D. L. Taylor. 1988. Analysis of rhodamine and fluorescein-labeled F-actin diffusion in vitro by fluorescence photobleaching recovery. *Biophys. J.* In press.

Soltys, B. J., and G. G. Borisy. 1985. Polymerization of tubulin in vivo: direct evidence for assembly onto microtubule ends and from centrosomes. *J. Cell Biol.* 100:1682–1689.

Stemple, D. L., S. C. Sweet, M. J. Welsh, and J. R. McIntosh. 1988. Dynamics of a fluorescent calmodulin analogue in the mammalian mitotic spindle at metaphase. *Cell Motil. Cytoskeleton.* 9:231–242.

Wadsworth, P., and E. D. Salmon. 1986. Microtubule dynamics of mitotic spindles of living cells. *Ann. NY Acad Sci.* 466:580–592.

Wadsworth, P., and R. D. Sloboda. 1983. Microinjection of fluorescent tubulin into dividing sea urchin cells. *J. Cell Biol.* 97:1249–1254.

Williams, R. C., and J. C. Lee. 1982. Preparation of tubulin from brain. *Methods Enzymol.* 85:376–385.